

Radial-flow fluctuations in the geometrical-scaling framework

Takeshi Osada*

*Department of Natural Sciences, Faculty of Science and Engineering,
Tokyo City University, Tamazutsumi 1-28-1, Setagaya-ku, Tokyo 158-8557, Japan.*

(Dated: June 2, 2026)

We discuss radial-flow fluctuations using the p_T -differential measure $v_0(p_T)$, together with its p_T -integrated counterpart v_0 , within the framework of geometrical scaling (GS), where the saturation momentum scale provides the characteristic scale for particle production. We show that the GS framework leads to results similar to those obtained from the momentum-rescaling model proposed by Jiangyong Jia. In the GS picture, event-by-event spectral fluctuations are governed by fluctuations of the saturation momentum scale; consequently, the single-mode ansatz introduced in Jia's model emerges naturally. We also show that the GS picture suggests a possible connection between transverse-momentum correlations and fluctuations of the emission region, which may be probed through Hanbury Brown and Twiss (HBT) analyses. Using the string percolation model, which is closely related to GS, we estimate the multiplicity dependence of radial-flow fluctuations and propose the scaled quantity $A_0(N_{\Delta y}) \equiv v_0^2 N_{\Delta y}$, with $N_{\Delta y} = (dN/dy)\Delta y$, as a diagnostic observable for testing the role of effective flux-tube fluctuations.

I. INTRODUCTION

Recent measurements by the ATLAS Collaboration [1] and the ALICE Collaboration [2] have revealed intriguing features in the behavior of the p_T -differential radial-flow fluctuation measure $v_0(p_T)$ [3]. In particular, the ratio $v_0(p_T)/v_0$, where v_0 is the p_T -integrated measure, exhibits a universal shape as a function of p_T . Although this behavior appears to be nearly universal, its physical origin has not yet been fully understood.

Jia [4] proposed a momentum-rescaling model that provides a possible baseline for the observed shape of $v_0(p_T)$. In this model, event-by-event spectral fluctuations are assumed to be driven by a single collective variable, namely the event-by-event mean transverse momentum. This assumption is formulated as a single-mode ansatz, in which the normalized spectral fluctuation is proportional to the fluctuation of the mean transverse momentum. While this ansatz successfully captures important features of the data, its physical origin remains to be clarified.

Geometrical scaling (GS) [5–8] provides a natural framework for addressing this issue. In the GS picture, the saturation momentum scale [9, 10] provides the characteristic momentum scale that governs transverse-momentum spectra. In particular, analyses of semi-inclusive transverse-momentum spectra in pp and p -Pb collisions have shown that spectra over a wide range of collision energies and multiplicities can be described in terms of a multiplicity-dependent saturation momentum scale [11–13]. If the GS framework is applicable to event-by-event spectral fluctuations in semi-inclusive events, the single-mode ansatz adopted in Jia's model can naturally be interpreted as arising from fluctuations of the saturation momentum scale, the characteristic momentum scale of the spectra.

In this paper, we show that the GS framework yields a factorized form analogous to Jia's momentum-rescaling model. The GS result for $v_0(p_T)$ provides a baseline associated only with saturation-scale fluctuations. Deviations from this baseline may signal additional fluctuation sources beyond saturation-scale fluctuations. We also discuss the relation between transverse-momentum correlations and fluctuations of the transverse emission region, suggesting a possible connection with HBT observables [14, 15]. Furthermore, the GS picture is known to be closely related to the string percolation model [16, 17]. In this model, fluctuations of the saturation momentum scale can be interpreted in terms of fluctuations of the string density. Using the string percolation picture, we estimate the multiplicity dependence of radial-flow fluctuations and discuss the expected scaling behavior of observables such as $v_0(p_T)$ and $A_0(N_{\Delta y}) \equiv v_0^2 N_{\Delta y}$, with $N_{\Delta y} = (dN/dy)\Delta y$. This provides a phenomenological link between GS, string-density fluctuations, and radial-flow fluctuation observables.

The paper is organized as follows. In Sec. II, we briefly introduce the framework of geometrical scaling for semi-inclusive transverse-momentum spectra. Then, we discuss how event-by-event fluctuations of produced particle spectra are related to fluctuations of the saturation momentum scale in semi-inclusive events. We then show that the spectral fluctuations obtained in the GS picture have the same single-mode structure as that assumed in Jia's model. In Sec. III, we derive the two-particle transverse-momentum correlation function within the GS framework. Furthermore, using the known multiplicity dependence of the saturation momentum scale, we discuss the expected p_T dependence and multiplicity dependence of $v_0(p_T)/v_0$. In Sec. IV, we use the string percolation model to estimate the multiplicity dependence of v_0 and related observables. Finally, Sec. V is devoted to a summary and concluding remarks.

* t-osada@tcu.ac.jp

II. TRANSVERSE-MOMENTUM FLUCTUATIONS IN THE GEOMETRICAL-SCALING FRAMEWORK

For each event multiplicity class, the semi-inclusive transverse momentum spectra of hadrons normalized by an effective cross-sectional area S_{T}^* can be scaled to a universal function

$$\frac{1}{S_{\text{T}}^*} \frac{dN}{2\pi p_{\text{T}} dp_{\text{T}} dy} = \mathcal{F}(\tau), \quad (1)$$

with scaling variable $\tau^{1/(2+\lambda)} = p_{\text{T}}/Q_{\text{sat}}$, where Q_{sat} is the multiplicity-dependent saturation momentum scale as a function of the effective energy W^* . The function $\mathcal{F}(\tau)$ represents the universal scaling function, for which a Tsallis-type form is often used in GS analyses [11]:

$$\mathcal{F}(\tau) = \left[1 + (q-1) \frac{\tau^{1/(2+\lambda)}}{\kappa} \right]^{\frac{-1}{q-1}}, \quad (2)$$

where q is the nonextensive parameter and κ is a constant relating Q_{sat} to a hadronization scale, such as the freeze-out temperature T_{f} . Denoting the event-by-event mean transverse momentum of produced charged particles by $[p_{\text{T}}]$, its event average within a fixed multiplicity class is given by

$$\langle [p_{\text{T}}] \rangle = \frac{2\kappa}{4-3q} \langle Q_{\text{sat}} \rangle. \quad (3)$$

Here, $\langle Q_{\text{sat}} \rangle$ denotes the event-averaged saturation momentum scale in a given semi-inclusive event class. Event-by-event fluctuations around this mean value are introduced below.

A. Fluctuations of the saturation momentum scale and the effective interaction area

Even within a semi-inclusive event class specified by the multiplicity, the event-by-event mean transverse momentum $[p_{\text{T}}]$ fluctuates from event to event. In the GS framework, as indicated by Eq. (3), this fluctuation can be understood as a fluctuation of the saturation momentum scale Q_{sat} . Denoting the saturation momentum scale averaged over events within a given semi-inclusive class by $\langle Q_{\text{sat}} \rangle$, we write the event-by-event saturation momentum scale as

$$Q_{\text{sat}} = \langle Q_{\text{sat}} \rangle + \delta Q_{\text{sat}}. \quad (4)$$

This saturation momentum scale is regarded as a function of the effective energy W^* in the collision:

$$Q_{\text{sat}}(W^*) = Q_0 \left(\frac{x_0 W^*}{Q_0} \right)^{\lambda/(2+\lambda)}. \quad (5)$$

Here, Q_0 , x_0 , and λ are the constants appearing in the saturation-momentum parametrization for inclusive

spectra [8, 18], and the collision energy W is replaced by the effective energy W^* . Thus, within this parametrization, fluctuations of the saturation momentum scale reflect fluctuations of the effective energy W^* . It is therefore natural to identify the mean saturation momentum scale entering the average spectrum of a semi-inclusive event class with the value evaluated at the mean effective energy $\langle W^* \rangle$:

$$\langle Q_{\text{sat}} \rangle = Q_{\text{sat}}(\langle W^* \rangle). \quad (6)$$

The mean transverse momentum of charged particles produced in each event is then given by

$$\begin{aligned} [p_{\text{T}}] &= \langle [p_{\text{T}}] \rangle + \delta [p_{\text{T}}] = \frac{2\kappa}{4-3q} (\langle Q_{\text{sat}} \rangle + \delta Q_{\text{sat}}) \\ &= \langle [p_{\text{T}}] \rangle \left(1 + \frac{\delta Q_{\text{sat}}}{\langle Q_{\text{sat}} \rangle} \right), \end{aligned} \quad (7)$$

where $\langle [p_{\text{T}}] \rangle$ denotes the average of the event-by-event mean transverse momentum over events in a given semi-inclusive class. It corresponds to the mean transverse momentum $\langle p_{\text{T}} \rangle$ for that semi-inclusive class. The corresponding transverse-momentum fluctuation is

$$\frac{\delta [p_{\text{T}}]}{\langle [p_{\text{T}}] \rangle} = \frac{\delta Q_{\text{sat}}}{\langle Q_{\text{sat}} \rangle} \approx \frac{\lambda}{2+\lambda} \frac{\delta W^*}{\langle W^* \rangle}. \quad (8)$$

Furthermore, for semi-inclusive transverse momentum spectra in the rapidity interval $-\Delta y/2 < y < +\Delta y/2$,

$$N(p_{\text{T}}) \equiv \frac{dN}{dp_{\text{T}} dy}, \quad (9)$$

the multiplicity in this interval, $N_{\Delta y} \equiv (dN/dy)\Delta y$, is fixed. Therefore,

$$N_{\Delta y} = \int dp_{\text{T}} N(p_{\text{T}}) = \frac{2\pi\kappa^2 \Delta y}{(2-q)(3-2q)} S_{\text{T}}^* Q_{\text{sat}}^2. \quad (10)$$

This relation implies a correlation between Q_{sat} and S_{T}^* . If fluctuations of the other spectral parameters, such as κ and q , can be neglected,

$$\frac{\delta S_{\text{T}}^*}{\langle S_{\text{T}}^* \rangle} = -2 \frac{\delta Q_{\text{sat}}}{\langle Q_{\text{sat}} \rangle}. \quad (11)$$

Thus, Eq. (11) shows that fluctuations of the saturation momentum scale are directly related to fluctuations of the effective area S_{T}^* .

B. Fluctuations of the transverse-momentum spectrum in the GS framework

The average transverse-momentum spectrum over a semi-inclusive event class, namely an ensemble of events satisfying a fixed multiplicity condition dN/dy around

midrapidity, may be approximated by using event-averaged saturation momentum $\langle Q_{\text{sat}} \rangle$ and the event-averaged effective area $\langle S_{\text{T}}^* \rangle$ as follows:

$$\begin{aligned} \langle N(p_{\text{T}}) \rangle &\approx N(p_{\text{T}}, \langle S_{\text{T}}^* \rangle, \langle Q_{\text{sat}} \rangle) \\ &= 2\pi p_{\text{T}} \langle S_{\text{T}}^* \rangle \left[1 + (q-1) \frac{p_{\text{T}}}{\kappa \langle Q_{\text{sat}} \rangle} \right]^{\frac{-1}{q-1}}. \end{aligned} \quad (12)$$

Note that, in general,

$$\langle N(p_{\text{T}}) \rangle \neq N(p_{\text{T}}, \langle S_{\text{T}}^* \rangle, \langle Q_{\text{sat}} \rangle). \quad (13)$$

This distinction should be noted when event-by-event fluctuations are included. The approximation becomes valid when the fluctuations around the mean spectrum are small and second-order effects in the spectral fluctuations can be neglected. Such second-order effects enter naturally in the two-particle correlation functions discussed below.

The spectrum in an event where the saturation momentum and the effective area fluctuate around their respective event-averaged values is written as

$$N(p_{\text{T}}) = N(p_{\text{T}}, \langle S_{\text{T}}^* \rangle + \delta S_{\text{T}}^*, \langle Q_{\text{sat}} \rangle + \delta Q_{\text{sat}}). \quad (14)$$

For each event, the mean transverse momentum of produced charged particles is given by Eq. (7). Assuming that the event-by-event deviation of the transverse-momentum spectrum from the event-averaged spectrum is small, we expand the spectral fluctuation to first order:

$$\begin{aligned} N(p_{\text{T}}) &\approx N(p_{\text{T}}, \langle S_{\text{T}}^* \rangle, \langle Q_{\text{sat}} \rangle) \\ &+ \left. \frac{\partial N(p_{\text{T}}, S_{\text{T}}^*, Q_{\text{sat}})}{\partial S_{\text{T}}^*} \right|_{\langle S_{\text{T}}^* \rangle, \langle Q_{\text{sat}} \rangle} \times \delta S_{\text{T}}^* \\ &+ \left. \frac{\partial N(p_{\text{T}}, S_{\text{T}}^*, Q_{\text{sat}})}{\partial Q_{\text{sat}}} \right|_{\langle S_{\text{T}}^* \rangle, \langle Q_{\text{sat}} \rangle} \times \delta Q_{\text{sat}} \\ &\approx \langle N(p_{\text{T}}) \rangle \left[1 + \frac{\frac{p_{\text{T}}}{\kappa \langle Q_{\text{sat}} \rangle}}{1 + (q-1) \frac{p_{\text{T}}}{\kappa \langle Q_{\text{sat}} \rangle}} \frac{\delta Q_{\text{sat}}}{\langle Q_{\text{sat}} \rangle} + \frac{\delta S_{\text{T}}^*}{\langle S_{\text{T}}^* \rangle} \right]. \end{aligned} \quad (15)$$

(For compactness, we use the notation $\dots|_{\langle S_{\text{T}}^* \rangle, \langle Q_{\text{sat}} \rangle}$ to indicate evaluation at $(S_{\text{T}}^*, Q_{\text{sat}}) = (\langle S_{\text{T}}^* \rangle, \langle Q_{\text{sat}} \rangle)$.) Using $\delta N(p_{\text{T}}) \equiv N(p_{\text{T}}) - \langle N(p_{\text{T}}) \rangle$ and Eq. (11), one obtains

$$\frac{\delta N(p_{\text{T}})}{\langle N(p_{\text{T}}) \rangle} \approx \left[\frac{\frac{p_{\text{T}}}{\kappa \langle Q_{\text{sat}} \rangle}}{1 + (q-1) \frac{p_{\text{T}}}{\kappa \langle Q_{\text{sat}} \rangle}} - 2 \right] \frac{\delta Q_{\text{sat}}}{\langle Q_{\text{sat}} \rangle}, \quad (16)$$

and using Eq. (7), this can also be written as

$$\frac{\delta N(p_{\text{T}})}{\langle N(p_{\text{T}}) \rangle} \approx \left[\frac{\frac{p_{\text{T}}}{\kappa \langle Q_{\text{sat}} \rangle}}{1 + (q-1) \frac{p_{\text{T}}}{\kappa \langle Q_{\text{sat}} \rangle}} - 2 \right] \frac{\delta[p_{\text{T}}]}{\langle [p_{\text{T}}] \rangle}. \quad (17)$$

C. Comparison with Jia's momentum-rescaling model

We now examine the same normalized spectral fluctuation using Jia's rescaling model. Here the event average is

again understood as an average over a multiplicity-fixed semi-inclusive event class. As assumed in Jia's rescaling model, the transverse-momentum spectrum observed in each event is determined by the event-by-event mean transverse momentum $[p_{\text{T}}]$ and by particle-number conservation. In other words, each event spectrum is generated from the ensemble-averaged spectrum by the rescaling

$$p_{\text{T}} \rightarrow p_{\text{T}} \frac{\langle [p_{\text{T}}] \rangle}{[p_{\text{T}}]},$$

together with the corresponding normalization factor. Following the notation of Jia [4], we introduce the event-wise normalized transverse-momentum spectrum [19] as

$$n(p_{\text{T}}) \equiv \frac{1}{N_{\Delta y}} N(p_{\text{T}}), \quad N_{\Delta y} \equiv \frac{dN}{dy} \Delta y, \quad (18)$$

where Δy is the width of the rapidity window. The event average of $n(p_{\text{T}})$ is denoted by

$$f(p_{\text{T}}) \equiv \langle n(p_{\text{T}}) \rangle = \frac{1}{N_{\Delta y}} \langle N(p_{\text{T}}) \rangle. \quad (19)$$

We assume that the spectrum in each event is generated by rescaling the transverse-momentum axis of the average spectrum $f(p_{\text{T}})$:

$$\begin{aligned} n(p_{\text{T}}) &= \frac{\langle [p_{\text{T}}] \rangle}{[p_{\text{T}}]} f\left(p_{\text{T}} \frac{\langle [p_{\text{T}}] \rangle}{[p_{\text{T}}]}\right) \\ &= \frac{1}{1 + \delta[p_{\text{T}}]/\langle [p_{\text{T}}] \rangle} f\left(\frac{p_{\text{T}}}{1 + \delta[p_{\text{T}}]/\langle [p_{\text{T}}] \rangle}\right). \end{aligned} \quad (20)$$

Here the prefactor $\langle [p_{\text{T}}] \rangle/[p_{\text{T}}] = 1/(1 + \delta[p_{\text{T}}]/\langle [p_{\text{T}}] \rangle)$ is introduced so that the normalization condition of the spectrum is preserved under the rescaling of the transverse-momentum axis:

$$\int dp_{\text{T}} n(p_{\text{T}}) = \int dp_{\text{T}} f(p_{\text{T}}) = 1. \quad (21)$$

Substituting the geometrical-scaling form of the average spectrum, Eq. (12), into the rescaling relation and expanding the resulting expression to first order in $\delta[p_{\text{T}}]/\langle [p_{\text{T}}] \rangle$, one obtains

$$\begin{aligned} n(p_{\text{T}}) &\approx \frac{2\pi p_{\text{T}} \langle S_{\text{T}}^* \rangle}{N_{\Delta y}} \left[1 + (q-1) \frac{p_{\text{T}}}{\kappa \langle Q_{\text{sat}} \rangle} \right]^{\frac{-1}{q-1}} \\ &\times \left[1 - 2 \frac{\delta[p_{\text{T}}]}{\langle [p_{\text{T}}] \rangle} \right] \left[1 + \frac{\frac{p_{\text{T}}}{\kappa \langle Q_{\text{sat}} \rangle}}{1 + (q-1) \frac{p_{\text{T}}}{\kappa \langle Q_{\text{sat}} \rangle}} \frac{\delta[p_{\text{T}}]}{\langle [p_{\text{T}}] \rangle} \right]. \end{aligned} \quad (22)$$

Therefore, the relative fluctuation of the transverse-momentum spectrum at fixed p_{T} , i.e., the vertical fluctuation, is obtained as

$$\frac{\delta n(p_{\text{T}})}{\langle n(p_{\text{T}}) \rangle} \approx \left[\frac{\frac{p_{\text{T}}}{\kappa \langle Q_{\text{sat}} \rangle}}{1 + (q-1) \frac{p_{\text{T}}}{\kappa \langle Q_{\text{sat}} \rangle}} - 2 \right] \frac{\delta[p_{\text{T}}]}{\langle [p_{\text{T}}] \rangle}. \quad (23)$$

This is identical to Eq. (17), which was derived for fluctuations of semi-inclusive transverse momentum spectra in the GS framework.

III. TWO-PARTICLE MOMENTUM CORRELATION AND RADIAL FLOW FLUCTUATIONS IN THE GS PICTURE

A. Two-particle transverse-momentum correlation

The correlation function of semi-inclusive transverse momentum spectra in the GS framework can be obtained directly from the spectral fluctuations. We define the correlation function as

$$\begin{aligned} C(p_{T1}, p_{T2}) &\equiv \frac{\langle N(p_{T1})N(p_{T2}) \rangle}{\langle N(p_{T1}) \rangle \langle N(p_{T2}) \rangle} - 1 \\ &= \frac{\langle \delta N(p_{T1}) \delta N(p_{T2}) \rangle}{\langle N(p_{T1}) \rangle \langle N(p_{T2}) \rangle}. \end{aligned} \quad (24)$$

Here, the GS spectral response function $K_{GS}(p_T)$ is defined as

$$K_{GS}(p_T) \equiv \frac{\frac{p_T}{\kappa \langle Q_{sat} \rangle}}{1 + (q-1) \frac{p_T}{\kappa \langle Q_{sat} \rangle}} - 2. \quad (25)$$

Using this definition together with Eq. (16), we obtain

$$C(p_{T1}, p_{T2}) = \frac{K_{GS}(p_{T1})K_{GS}(p_{T2})}{\langle Q_{sat} \rangle^2} \langle (\delta Q_{sat})^2 \rangle. \quad (26)$$

Equation (26) indicates that the correlation function of semi-inclusive transverse momentum spectra in the GS framework is determined by the magnitude of the saturation momentum fluctuation, $\langle (\delta Q_{sat})^2 \rangle$, and by the spectral response function $K_{GS}(p_T)$.

Since Eq. (11) holds in semi-inclusive events, if we define a size scale of the effective area by $R_T^* \equiv \sqrt{S_T^*/\pi}$, then the fluctuation of R_T^* is related to the fluctuation of Q_{sat} as

$$\frac{\delta R_T^*}{\langle R_T^* \rangle} = - \frac{\delta Q_{sat}}{\langle Q_{sat} \rangle}. \quad (27)$$

Thus, in the GS framework, the transverse-momentum correlation function is also related to fluctuations of the size scale associated with the effective area:

$$C(p_{T1}, p_{T2}) = K_{GS}(p_{T1})K_{GS}(p_{T2}) \frac{\langle (\delta R_T^*)^2 \rangle}{\langle R_T^* \rangle^2}. \quad (28)$$

The quantity $\langle (\delta R_T^*)^2 \rangle / \langle R_T^* \rangle^2$ is expected to be constrained, for example, through HBT analyses of the emission region. Although R_T^* is not identical to an HBT radius, the GS picture predicts a possible connection between transverse-momentum correlations and fluctuations of the emission region inferred from HBT measurements [14, 15]:

$$\frac{\langle (\delta R_T^*)^2 \rangle}{\langle R_T^* \rangle^2} = \frac{C(p_{T1}, p_{T2})}{K_{GS}(p_{T1})K_{GS}(p_{T2})}. \quad (29)$$

Thus, the GS picture suggests that the spectral correlation function is connected not only to saturation-scale

fluctuations but also to fluctuations of the effective transverse area. The corresponding size scale, R_T^* , however, should not be identified directly with the HBT radius R_{HBT} . Clarifying the relation between these two quantities remains an important subject for future study.

B. p_T -differential and -integrated measure of radial-flow fluctuations

The p_T -differential measure of radial-flow fluctuations, $v_0(p_T)$, quantifies the component of the yield fluctuation at a given p_T that is correlated with the event-by-event mean transverse momentum $[p_T]$. The p_T -differential measure $v_0(p_T)$ is defined as

$$\begin{aligned} v_0(p_T) &\equiv \rho(N(p_T), [p_T]) \frac{\sqrt{\langle (\delta N(p_T))^2 \rangle}}{\langle N(p_T) \rangle}, \\ &= \frac{\langle \delta N(p_T) \delta [p_T] \rangle}{\langle N(p_T) \rangle \sqrt{\langle (\delta [p_T])^2 \rangle}}, \end{aligned} \quad (30)$$

where

$$\rho(N(p_T), [p_T]) \equiv \frac{\langle \delta N(p_T) \delta [p_T] \rangle}{\sqrt{\langle (\delta N(p_T))^2 \rangle \langle (\delta [p_T])^2 \rangle}} \quad (31)$$

is the Pearson correlation coefficient between the spectrum fluctuation $\delta N(p_T)$ and the mean transverse momentum fluctuation $\delta [p_T]$. In the geometrical-scaling framework, this correlation can be interpreted as the response of the spectrum to event-by-event fluctuations of the saturation momentum scale Q_{sat} . This interpretation is supported by the fact that, to leading order in δQ_{sat} , one obtains

$$\langle \delta N(p_T) \delta [p_T] \rangle = \langle N(p_T) \rangle \langle [p_T] \rangle K_{GS}(p_T) \frac{\langle (\delta Q_{sat})^2 \rangle}{\langle Q_{sat} \rangle^2}. \quad (32)$$

In this approximation, both $\delta N(p_T)$ and $\delta [p_T]$ are driven by the same event-by-event fluctuation δQ_{sat} . Therefore, the magnitude of the Pearson correlation coefficient is unity,

$$|\rho(N(p_T), [p_T])| = 1, \quad (33)$$

while its sign is determined by $K_{GS}(p_T)$. Substituting the above covariance into the definition of $v_0(p_T)$, we obtain

$$v_0(p_T) = K_{GS}(p_T) \frac{\sqrt{\langle (\delta Q_{sat})^2 \rangle}}{\langle Q_{sat} \rangle}. \quad (34)$$

The relation $|\rho(N(p_T), [p_T])| = 1$ means that the spectral fluctuation and the mean-transverse-momentum fluctuation are perfectly correlated or anticorrelated. In the present GS picture, both originate from the same physical source, namely the event-by-event fluctuation of the saturation momentum scale Q_{sat} . This also implies that

$v_0(p_T)$ is determined by the spectral response function $K_{\text{GS}}(p_T)$ and by the magnitude of the saturation-scale fluctuation, $\sqrt{\langle(\delta Q_{\text{sat}})^2\rangle}/\langle Q_{\text{sat}}\rangle$. On the other hand, the p_T -integrated measure v_0 is defined as

$$v_0 \equiv \int dp_T \left[\frac{p_T - \langle p_T \rangle}{\langle p_T \rangle} \right] v_0(p_T) \langle n(p_T) \rangle \\ = \frac{\sqrt{\langle(\delta[p_T])^2\rangle}}{\langle p_T \rangle} = \frac{\sqrt{\langle(\delta Q_{\text{sat}})^2\rangle}}{\langle Q_{\text{sat}} \rangle}. \quad (35)$$

Therefore,

$$\frac{v_0(p_T)}{v_0} = K_{\text{GS}}(p_T). \quad (36)$$

In the GS picture, we therefore obtain

$$\frac{\delta n(p_T)}{\langle n(p_T) \rangle} = K_{\text{GS}}(p_T) \frac{\delta[p_T]}{\langle p_T \rangle} \\ = \frac{v_0(p_T)}{v_0} \frac{\delta[p_T]}{\langle p_T \rangle}. \quad (37)$$

This is precisely the single-mode ansatz assumed by Jia in the rescaling model [Eq. (2) of Ref. [4]]. Thus, in the minimal GS picture considered here, the single-mode ansatz is not an additional assumption but follows naturally when the dominant fluctuation source is the saturation momentum scale.

C. GS baseline for $v_0(p_T)/v_0$

We now examine the ratio of the p_T -differential and p_T -integrated measures, $v_0(p_T)/v_0$, obtained in the GS picture. From Eq. (36), this ratio reduces simply to $K_{\text{GS}}(p_T)$, namely the quantity defined in Eq. (25) as a function of p_T . For semi-inclusive events, this result represents the contribution arising solely from fluctuations of the saturation momentum scale. Therefore, deviations of the measured $v_0(p_T)/v_0$ from $K_{\text{GS}}(p_T)$ may indicate the presence of fluctuation sources not accounted for by saturation-scale fluctuations. In this sense, $K_{\text{GS}}(p_T)$ can serve as a baseline for isolating such additional contributions.

According to our previous work [11], the saturation momentum scale Q_{sat} and the effective interaction size scale R_{T}^* depend on the multiplicity fixed in the semi-inclusive event class, namely the value of dN/dy at midrapidity. They can be parametrized as

$$Q_{\text{sat}} = a_Q + b_Q \left(\frac{dN}{dy} \right)^{1/6}, \quad (38a)$$

$$R_{\text{T}}^* = a_R + b_R \left(\frac{dN}{dy} \right)^{1/3}. \quad (38b)$$

The values of a_Q , b_Q , a_R , and b_R for pp and p -Pb collisions at several collision energies are listed in Table I.

TABLE I. Parameters used to parametrize the multiplicity-dependent saturation momentum Q_{sat} according to Eq. (38a). In the numerical estimate, we use $q = 1.145$ and $\kappa = 0.1100$, which are the values of the universal function used for the GS analysis of semi-inclusive π^\pm spectra in pp and p -Pb collisions. The values are reproduced in part from Table II of Ref. [11].

System and energy	a_Q	b_Q
$pp \rightarrow \pi^\pm + X$		
2.76 TeV [20]	-0.019	0.854
7.00 TeV [20]	-0.149	0.954
7.00 TeV [21]	-0.225	0.985
13.0 TeV [22]	-0.472	1.164
p -Pb $\rightarrow \pi^\pm + X$		
5.02 TeV [23]	0.078	0.899
5.02 TeV [24]	0.315	0.600

As representative examples, we consider $pp \rightarrow \pi^\pm + X$ at $\sqrt{s} = 7.00$ TeV [21] and p -Pb $\rightarrow \pi^\pm + X$ at $\sqrt{s} = 5.02$ TeV [23]. The resulting K_{GS} is shown in Fig. 1. As shown in Fig. 1, $K_{\text{GS}}(p_T)$ starts from a negative value at low p_T , crosses zero at around $p_T \simeq 0.5$ – 0.7 GeV/ c , and increases monotonically with increasing p_T . [25] The obtained GS spectral response function exhibits a similar p_T dependence for pp and p -Pb collisions, suggesting a universal character of the response function within the present GS framework.

It should be emphasized that the present minimal GS baseline does not produce the high- p_T falloff observed in heavy-ion collision data. Rather, it accounts for the sign change and the low- p_T rise of $v_0(p_T)/v_0$ associated with the spectral response to saturation-scale fluctuations. A deviation of the measured $v_0(p_T)/v_0$ from this monotonic baseline, especially at high p_T , may indicate the presence of additional fluctuation sources, such as those arising from jet production or other hard processes, which are not included in the minimal GS picture.

IV. RELATION TO THE STRING PERCOLATION MODEL

The string percolation model (see Refs. [16, 17] and the Appendix of Ref. [11]) also predicts that the spectral fluctuation and the mean-transverse-momentum fluctuation are strongly correlated, in close analogy with the GS picture.

The area covered by strings is given by $S_{\text{T}}^*(1 - e^{-\eta})$, where $S_{\text{T}}^*e^{-\eta}$ represents the uncovered area. The average number of effective color flux tubes is then estimated by dividing this covered area by the area of an effective string, $\sigma_1 F(\eta)$:

$$\langle N_{\text{eff}} \rangle = \frac{S_{\text{T}}^*(1 - e^{-\eta})}{\sigma_1 F(\eta)}. \quad (39)$$

Here, η is the mean string density, defined as $\eta = N_s \sigma_1 / S_{\text{T}}^*$, with N_s being the number of strings. The area

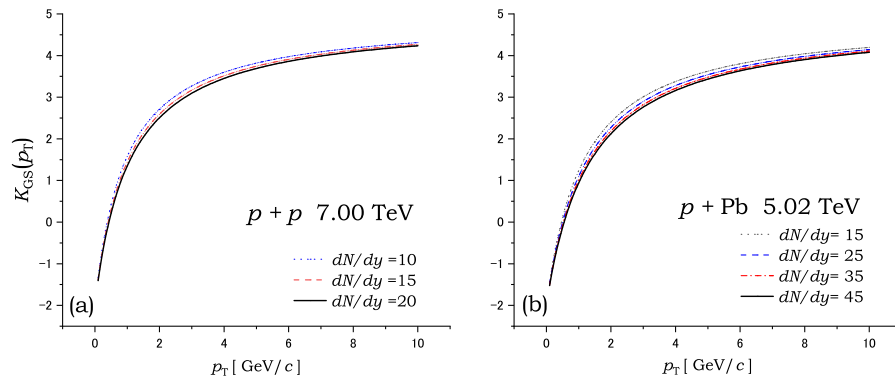


FIG. 1. Baseline estimate of $K_{\text{GS}}(p_{\text{T}})$ for pp and p -Pb collisions obtained from the geometric-scaling parametrization. The Tsallis parameters $q = 1.145$ and $\kappa = 0.1100$ are fixed to the values used in Table I. The curves represent the spectral response to fluctuations of Q_{sat} within the GS framework, with no additional dynamical fluctuation sources included.

of a single string is denoted by σ_1 , and the factor $F(\eta)$ accounts for the reduction of the effective string area due to the overlap of strings in the transverse plane, which is given by

$$F(\eta) = \sqrt{\frac{1 - e^{-\eta}}{\eta}}. \quad (40)$$

The quantity $\langle N_{\text{eff}} \rangle$ may be regarded as the counterpart of $S_{\text{T}}^* Q_{\text{sat}}^2$, which represents the average number of color flux tubes in the GS picture. Equating these two quantities gives

$$Q_{\text{sat}}^2 = \frac{\sqrt{\eta(1 - e^{-\eta})}}{\sigma_1} \propto \begin{cases} \eta, & \eta \ll 1, \\ \sqrt{\eta}, & \eta \gg 1. \end{cases} \quad (41)$$

In the high-density limit $\eta \gg 1$, the effective energy dependence of the mean string density η may be estimated as

$$\eta = (\sigma_1 Q_0^{\frac{2}{2+\lambda}})^2 W^{* \frac{2\lambda}{2+\lambda}}, \quad (42)$$

and, for $\lambda = 0.22$, one obtains $\eta \sim (W^*)^{1/5}$. The fluctuation of the saturation momentum scale can then be related to the fluctuation of the string density η as

$$\frac{\delta Q_{\text{sat}}}{\langle Q_{\text{sat}} \rangle} = \frac{\alpha(\eta)}{4} \frac{\delta \eta}{\eta}, \quad (43)$$

where $\alpha(\eta)$ is a function of η defined as

$$\alpha(\eta) \equiv 1 + \frac{\eta e^{-\eta}}{1 - e^{-\eta}}, \quad (44)$$

$$\alpha(\eta) \rightarrow \begin{cases} 2, & \eta \ll 1, \\ 1, & \eta \gg 1. \end{cases}$$

As shown in Eq. (43), the string percolation model also leads to a strong correlation between the spectral fluctuation and the mean-transverse-momentum fluctuation

via the common source of the fluctuation of the saturation momentum scale δQ_{sat} . Hence, using Eqs. (16) and (43), the relative fluctuation of the spectrum at fixed p_{T} can be expressed as

$$\frac{\delta N(p_{\text{T}})}{\langle N(p_{\text{T}}) \rangle} = K_{\text{GS}}(p_{\text{T}}) \frac{\alpha(\eta)}{4} \frac{\delta \eta}{\eta}. \quad (45)$$

Squaring Eq. (43) and taking the event average gives

$$\left\langle \left(\frac{\delta Q_{\text{sat}}}{Q_{\text{sat}}} \right)^2 \right\rangle = \frac{\alpha^2(\eta)}{16} \left\langle \left(\frac{\delta \eta}{\eta} \right)^2 \right\rangle. \quad (46)$$

If the fluctuations of the string density are governed by the finite number of effectively independent flux tubes, N_{eff} , the relative variance is expected to scale as

$$\left\langle \left(\frac{\delta \eta}{\eta} \right)^2 \right\rangle \sim \frac{1}{N_{\text{eff}}}, \quad (47)$$

and then we have

$$\left\langle \left(\frac{\delta Q_{\text{sat}}}{Q_{\text{sat}}} \right)^2 \right\rangle \sim \frac{\alpha^2(\eta)}{16 N_{\text{eff}}}. \quad (48)$$

This relation provides a simple estimate of the magnitude of saturation-scale fluctuations in terms of the number of effectively independent flux tubes. In the geometric-scaling description of semi-inclusive spectra, the multiplicity $N_{\Delta y}$ is given by Eq. (10). Since the number of effective flux tubes is also estimated as $N_{\text{eff}} \sim S_{\text{T}}^* Q_{\text{sat}}^2$, we may write phenomenologically

$$N_{\text{eff}} = C_{\text{eff}} N_{\Delta y}, \quad (49)$$

where C_{eff} is an unknown constant of order unity. This constant absorbs the difference between the number of effective flux tubes and the observed charged-particle multiplicity. Therefore,

$$\left\langle \left(\frac{\delta Q_{\text{sat}}}{Q_{\text{sat}}} \right)^2 \right\rangle \sim \frac{\alpha^2(\eta)}{16 C_{\text{eff}} N_{\Delta y}}. \quad (50)$$

In the geometric-scaling picture, the integrated radial-flow fluctuation v_0 may then be estimated as

$$v_0^2 \equiv \left\langle \left(\frac{\delta[p_T]}{\langle [p_T] \rangle} \right)^2 \right\rangle \simeq \left\langle \left(\frac{\delta Q_{\text{sat}}}{Q_{\text{sat}}} \right)^2 \right\rangle. \quad (51)$$

Thus, we obtain the following estimate for v_0^2 :

$$v_0^2 \sim \frac{\alpha^2(\eta)}{16C_{\text{eff}}} \frac{1}{N_{\Delta y}}. \quad (52)$$

This motivates the following scaled observable:

$$A_0(N_{\Delta y}) \equiv v_0^2 N_{\Delta y}. \quad (53)$$

In the string percolation picture, however, A_0 can be suppressed at high multiplicity through the density dependence of $\alpha(\eta)$, which reflects the nonlinear reduction associated with string fusion or percolation.

$$A_0(N_{\Delta y}) \sim \frac{\alpha^2(\eta)}{16 C_{\text{eff}}} = \begin{cases} \frac{1}{4C_{\text{eff}}}, & N_{\Delta y} \sim 1 \ (\eta \ll 1), \\ \frac{1}{16C_{\text{eff}}}, & N_{\Delta y} \gg 1 \ (\eta \gg 1). \end{cases} \quad (54)$$

Thus, the observable $A_0(N_{\Delta y})$ is a useful diagnostic quantity. If the system is described by a simple independent-source picture with a fixed relation between N_{eff} and multiplicity, this quantity should be approximately constant. On the other hand, if the system evolves from the low-density regime, $Q_{\text{sat}}^2 \propto \eta$, to the high-density percolated regime, $Q_{\text{sat}}^2 \propto \sqrt{\eta}$, then one expects a suppression of $v_0^2 N_{\Delta y}$ toward high multiplicity. In the simplest estimate, the high-density value is smaller than the low-density value by a factor of four:

$$\frac{[A_0(N_{\Delta y})]_{N_{\Delta y} \gg 1}}{[A_0(N_{\Delta y})]_{N_{\Delta y} \sim \mathcal{O}(1)}} \sim \frac{1}{4}. \quad (55)$$

This behavior would indicate the nonlinear reduction of density fluctuations associated with string fusion or percolation.

V. SUMMARY AND CONCLUDING REMARKS

We have discussed radial-flow fluctuations in the framework of geometrical scaling. In semi-inclusive event classes with fixed multiplicity, fluctuations of the saturation momentum scale Q_{sat} are correlated with fluctuations of the effective interaction area S_{T}^* . As a consequence, the spectral fluctuation of the transverse-momentum spectrum at fixed p_{T} can be written in terms

of a single fluctuation mode, $\delta Q_{\text{sat}}/\langle Q_{\text{sat}} \rangle$, which is directly related to the mean-transverse-momentum fluctuation $\delta[p_{\text{T}}]/\langle [p_{\text{T}}] \rangle$. This structure is precisely the single-mode ansatz assumed by Jia in the momentum-rescaling model [4]. Thus, the GS picture provides a natural explanation for the single-mode structure of radial-flow fluctuations. The spectral response function $K_{\text{GS}}(p_{\text{T}})$ then serves as a baseline for isolating additional contributions to radial-flow fluctuations beyond those arising from saturation-scale fluctuations.

We have also discussed the two-particle transverse-momentum correlation function in the GS framework. The correlation function factorizes into the product of $K_{\text{GS}}(p_{\text{T}1})$ and $K_{\text{GS}}(p_{\text{T}2})$, multiplied by the variance of the saturation-momentum fluctuation, $\langle (\delta Q_{\text{sat}})^2 \rangle / \langle Q_{\text{sat}} \rangle^2$. Through the fixed-multiplicity constraint, this variance is also related to fluctuations of the effective transverse size. This result suggests a possible connection between transverse-momentum correlations and fluctuations of the emission region inferred from HBT measurements.

Finally, we have discussed the relation between the GS picture and the string percolation model. In this picture, saturation-scale fluctuations can be interpreted as fluctuations of the string density η . Assuming that the relative variance of the string density is governed by the number of effective flux tubes, N_{eff} , we obtained a simple estimate of the magnitude of saturation-scale fluctuations in terms of N_{eff} . This estimate motivates the scaled observable

$$A_0(N_{\Delta y}) \equiv v_0^2 N_{\Delta y}, \quad N_{\Delta y} = \frac{dN}{dy} \Delta y,$$

which is expected to be approximately constant in a simple independent-source picture, but can be suppressed at high multiplicity in the string percolation picture due to the nonlinear reduction of density fluctuations associated with string fusion or percolation. The measurement of $A_0(N_{\Delta y})$ and its multiplicity dependence would provide a useful diagnostic for understanding the underlying physics of radial-flow fluctuations and the possible role of string percolation in high-energy collisions.

The present GS baseline should be regarded as the minimal spectral response generated by saturation-scale fluctuations at fixed multiplicity. Therefore, a comparison of this baseline with the measured $v_0(p_{\text{T}})/v_0$ can isolate deviations that are not accounted for by the GS response alone. Such deviations may provide insight into the presence of additional fluctuation sources beyond saturation-scale fluctuations, and may contain information about the dynamics of multiparticle production and possible final-state effects reflected in the observed spectra and correlations.

[1] G. Aad *et al.* (ATLAS), Evidence for the Collective Nature of Radial Flow in Pb+Pb Collisions with the

ATLAS Detector, Phys. Rev. Lett. **136**, 032301 (2026),

- arXiv:2503.24125 [nucl-ex].
- [2] S. Acharya *et al.* (ALICE), Long-range transverse momentum correlations and radial flow in Pb–Pb collisions at the LHC, *Phys. Rev. Lett.* **136**, 032302 (2026), arXiv:2504.04796 [nucl-ex].
- [3] A. Mazeliauskas and D. Teaney, Fluctuations of harmonic and radial flow in heavy ion collisions with principal components, *Phys. Rev. C* **93**, 024913 (2016), arXiv:1509.07492 [nucl-th].
- [4] J. Jia, Sources of Radial-Flow Fluctuations in the Quark-Gluon Plasma, *Phys. Rev. Lett.* **136**, 112301 (2026), arXiv:2507.14399 [nucl-th].
- [5] A. M. Stasto, K. J. Golec-Biernat, and J. Kwiecinski, Geometric scaling for the total $\gamma^* p$ cross-section in the low x region, *Phys. Rev. Lett.* **86**, 596 (2001), arXiv:hep-ph/0007192.
- [6] E. Iancu, K. Itakura, and L. McLerran, Geometric scaling above the saturation scale, *Nucl. Phys. A* **708**, 327 (2002), arXiv:hep-ph/0203137.
- [7] E. Iancu, K. Itakura, and L. McLerran, Geometric scaling in the color glass condensate, *Nucl. Phys. A* **721**, 293 (2003).
- [8] L. McLerran and M. Praszalowicz, Geometrical Scaling and the Dependence of the Average Transverse Momentum on the Multiplicity and Energy for the ALICE Experiment, *Phys. Lett. B* **741**, 246 (2015), arXiv:1407.6687 [hep-ph].
- [9] D. Kharzeev and E. Levin, Manifestations of high density QCD in the first RHIC data, *Phys. Lett. B* **523**, 79 (2001), arXiv:nucl-th/0108006.
- [10] F. Gelis, E. Iancu, J. Jalilian-Marian, and R. Venugopalan, The Color Glass Condensate, *Ann. Rev. Nucl. Part. Sci.* **60**, 463 (2010), arXiv:1002.0333 [hep-ph].
- [11] T. Osada, Multiplicity-dependent saturation momentum in p -Pb collisions at 5.02 TeV, *Phys. Rev. C* **103**, 024911 (2021), arXiv:2011.00456 [nucl-th].
- [12] T. Osada and T. Kumaoka, Saturation momentum scale extracted from semi-inclusive transverse spectra in high-energy pp collisions, *Phys. Rev. C* **100**, 034906 (2019), arXiv:1904.10823 [hep-ph].
- [13] T. Osada and M. Ishihara, Event-by-event mean p_T fluctuations and transverse size of color flux tube generated in p - p collisions at $\sqrt{s}=0.90$ TeV, *J. Phys. G* **45**, 015104 (2018), arXiv:1702.07440 [hep-ph].
- [14] C. Plumberg and U. Heinz, Probing the properties of event-by-event distributions in Hanbury-Brown–Twiss radii, *Phys. Rev. C* **92**, 044906 (2015), [Addendum: *Phys. Rev. C* **92**, 049901 (2015)], arXiv:1507.04968 [nucl-th].
- [15] C. Plumberg and U. Heinz, Observable consequences of event-by-event fluctuations of HBT radii, *Nucl. Phys. A* **956**, 381 (2016), arXiv:1512.07631 [nucl-th].
- [16] J. Dias de Deus and C. Pajares, String Percolation and the Glasma, *Phys. Lett. B* **695**, 211 (2011), arXiv:1011.1099 [hep-ph].
- [17] M. A. Braun, F. Del Moral, and C. Pajares, Percolation of strings and the first RHIC data on multiplicity and transverse momentum distributions, *Phys. Rev. C* **65**, 024907 (2002), arXiv:hep-ph/0105263.
- [18] K. J. Golec-Biernat and M. Wusthoff, Saturation effects in deep inelastic scattering at low Q^{*2} and its implications on diffraction, *Phys. Rev. D* **59**, 014017 (1998), arXiv:hep-ph/9807513.
- [19] Since the multiplicity is fixed in a semi-inclusive event class, $N(p_T)$ and the normalized spectrum $n(p_T)$ differ only by an overall constant. We therefore use $N(p_T)$ in the definition of $v_0(p_T)$ below, while the corresponding single-mode relation is equivalently written for $n(p_T)$.
- [20] S. Chatrchyan *et al.* (CMS), Study of the Inclusive Production of Charged Pions, Kaons, and Protons in pp Collisions at $\sqrt{s} = 0.9, 2.76,$ and 7 TeV, *Eur. Phys. J. C* **72**, 2164 (2012), arXiv:1207.4724 [hep-ex].
- [21] S. Acharya *et al.* (ALICE), Multiplicity dependence of light-flavor hadron production in pp collisions at $\sqrt{s} = 7$ TeV, *Phys. Rev. C* **99**, 024906 (2019), arXiv:1807.11321 [nucl-ex].
- [22] A. M. Sirunyan *et al.* (CMS), Measurement of charged pion, kaon, and proton production in proton-proton collisions at $\sqrt{s} = 13$ TeV, *Phys. Rev. D* **96**, 112003 (2017), arXiv:1706.10194 [hep-ex].
- [23] S. Chatrchyan *et al.* (CMS), Study of the Production of Charged Pions, Kaons, and Protons in pPb Collisions at $\sqrt{s_{NN}} = 5.02$ TeV, *Eur. Phys. J. C* **74**, 2847 (2014), arXiv:1307.3442 [hep-ex].
- [24] B. B. Abelev *et al.* (ALICE), Multiplicity Dependence of Pion, Kaon, Proton and Lambda Production in p-Pb Collisions at $\sqrt{s_{NN}} = 5.02$ TeV, *Phys. Lett. B* **728**, 25 (2014), arXiv:1307.6796 [nucl-ex].
- [25] It should be noted that the zero-crossing point is not determined solely by the spectral response itself, but can also be affected by analysis conventions, such as the finite p_T range used to define v_0 and the normalization of the event-by-event spectra.